Innovative: International Multi-disciplinary Journal of Applied Technology
(ISSN 2995-486X) VOLUME 02 ISSUE 11, 2024

Evaluation of Silver Nanoparticles Stabilized with Sulfurized Ligands as Mercury (Hg II) Sensors in Water Samples

Muhammed Abdel Hasan Shallal
Lecturer, M.Sc, Chemistry Field, Educational Directorate Thi-Qar, Thi-Qar, Iraq

Abstract:

In recent decades, Silver nanoparticles (SNPs) have attracted significant attention from the scientific community due to their distinctive property of localized surface Plasma resonance observed by Ultraviolet–visible spectroscopy. This relatively simple technique does not require sophisticated or instrumentation. Nanoparticles (NPs), unlike common dyes, have better stability, selectivity and viability characteristics to be very versatile, which allows these nanoparticles to be used as quite sensitive colorimetric sensors for the detection of Hg (II) ion, being able to form amalgams or aggregate. The proposed work aimed to prepare and evaluate colorimetric sensors based on SNPs for detecting mercury Hg (II) in water and to synthesize SNPs and characterize them using UV-Vis spectrophotometry. The protocol for synthesizing spherical SNPs was standardized by the modified process of the Creighton method. SNPs with an average diameter of 30±2 nm were obtained according to the characterization by analysis of the TEM images. A functionalization protocol for SNPs with cysteamine (Cy) and cysteine ligands for detecting Hg (II) ions in water was implemented and optimized. A protocol for quantifying Hg (II) ions in water by UV-Vis spectrophotometry was established and optimized for each sensor under study. It was possible to obtain a detection limit of 109 nm for the SNPs-CyNH2 sensor with an incubation time of 2 min and a detection limit of 445 nm the SNPs-Cy sensor with an incubation Of 20 min The sensor-based on SNPs-CyNH2 presents good selectivity for most of the interfering ions studied.

Keywords: Silver Nanoparticles, Mercury Sensors, Characteri2zation, modelling.

1.0 Introduction

Mercury has been widely studied as an environmental contaminant for several decades because it is a bio accumulative species, it is considered the most toxic heavy metal, and it is found everywhere in the environment and biota [1-3]. Of the different forms (II) is the most common and stable and

due to its solubility in water, it is capable of contaminating large volumes of water. When mercury is introduced into aquatic ecosystems, it can enter the marine food chain and accumulate to higher levels [4]. Therefore, monitoring Hg (II) levels in aquatic ecosystems even at low concentrations turns out to be very important. Some research groups such as Rajkumar et [5] have presented a selective colorimetric probe for the detection of Hg (II) that uses SNPs modified with cysteine. In this study, surface-enhanced Raman scattering (SERS) demonstrated that cysteine is bound to the surface of SNPs through the thiol with the carboxylate group pointing outwards. Furthermore, they observed that in the presence of Hg (II) the absorption peak decreases, resulting in a color change due to the interaction between SNPs and Hg (II), which causes the total disappearance of the LSPR peak. On the other hand, Chakraborty et al. [6] have developed a selective colorimetric sensor for Hg (II) in water, based on the functionalization of SNPs with cysteamine. showed that cysteamine molecules are bound to SNPs through the thiol group, leaving the amino group exposed. In addition, they proposed a mechanism for detecting Hg (II) by SNPs modified with cysteamine.

To date, variety of (II) detection methods that have been reported in the literature [1, 11, 12], among the most common is atomic absorption spectroscopy. These methods provide satisfactory limits of detection (LODs) at the ppb level, below the EPA-mandated maximum limit of 2 ppb (10 nm) for (II) in drinking water, however, they perform sophisticated, time-consuming, cost-intensive operations. Therefore, it would be desirable to have selective detection systems for (II) that are simpler, faster, more sensitive and more profitable. Thus, in recent decades SNPs and Ag NPs have attracted great attention from the scientific community due to their distinctive property of localized surface plasmon resonance observed by UV-Vis spectrophotometry, which is a relatively simple technique that does not requires sophisticated instrumentation. These nanoparticles can be Utilized as sensitive colorimetric sensors for the detection of Hg (II) because they have greater stability, selectivity, and survivability qualities than conventional dyes, which allow these nanoparticles to form amalgams or agglomerate. SNP-based colorimetric sensors for the detection of (II) were developed and tested in this study.

2.0 Materials and Methods

Reagents and Materials: The reagents used during this from Fisher Scientific, Sigma-Aldrich and Merck companies with AR grade 98% purity. On the other hand, it should be specified that the water used in all the experiments was ultrapure obtained from the Thermo Scientific ultrapure with pH 7.02.

2.2 Equipment: Perkin Elmer Lambda 850 UV-Visible Spectrophotometer, Agilent 8453 UV-Visible Spectrophotometer, AND GH200 model analytical balance, Elcio pH meter LI 120 model-Vortex Mixing Agitator – REMI 2 - MLH Magnetic Stirrers (with Hotplate and Sigma 1-16 centrifuge, has a maximum capacity of 24 microtubes and can reach speeds of 200 – 15000 rpm, with a built-in timer.

2.1 Methodology

Synthesis of silver nanoparticles (SNPs): The synthesis of the SNPs was carried out with a modification of the method of Creighton et al [7]. The process consisted of dissolving 1.7 mg of silver nitrate in 100 mL of ultrapure water in a 250 mL flask. Next, the silver nitrate solution was placed in an ice bath for 30 min until reaching a temperature of 2°C, under constant magnetic stirring at 500 rpm. Next, the sodium borohydride solution (1.5 mg in 700 μL) was added And prepared instantly by dissolving $NaBH_4$ with cold water, in aliquots of 20 μL. When the $NaBH_4$ solution was completely added, the container was removed from the ice bath and left under constant stirring until the solution reached room temperature.

Functionalization protocol of SNPs with cysteamine: Once the SNPs were synthesized, the pH was adjusted to 4 with a 0.1 M HCl solution. Then, under constant stirring, the $CyNH_2$ solution (0.3 mg of $CyNH_2$ in 1 mL of ultrapure water, 3.9 mM) was added dropwise and left under stirring for 1

hour. Afterward the excess ligand that could be in the solution was eliminated by means of centrifugation (9000 rpm for 30 min), the supernatant liquid was eliminated and the colloid was resuspended with ultrapure water adjusted to pH 4. This solution was stored at room temperature in a container protected from light, for when it was used in the characterization and subsequent tests. For the functionalization, the notation x5, x10 x 20 have been used, which refers to the volume of ligand to be used according to the notation x1 defined for 62.5 μL of ligand for every 25 mL of SNPs.

Functionalization protocol of SNPs with cysteine: Having previously performed the synthesis of the SNPs, the (Cy) solution (0.399 mg of $CyNH_2$ in 1 mL of ultrapure water, 3.3 mM) was added dropwise and left under stirring for 1 hour. ligand was then removed from the solution by centrifugation (9000 rpm for 30 min), removing the supernatant liquid and resuspending the colloid with ultrapure water adjusted to pH 8. This solution was stored at room temperature in a container protected from light. , for when it was used in the characterization and subsequent tests. For the functionalization, the notation 5, x10, 20 has been used, which refers to the volume of ligand to be used according to the notation ×1 defined for 62.5 μL of ligand for every 25 mL of SNPs.

Characterization of SNPs by UV-Vis spectroscopy: The characterization of newly synthesized SNPs or functionalized with $CyNH_2$ or Cy was performed by UV spectroscopy, by means of the wavelength at which the characteristic LSPR for spherical SNPs appeared. Experimentally, 1 mL of the NPs was taken and measured in the spectrophotometer, scanning between 300-700 nm.

Characterization of SNPs by TEM microscopy: For TEM measurements, a few microliter aliquot of the colloid placed on a carbon-coated copper grid and dried at room temperature. TEM images were taken using a TEM (model TECNAI G^2 TF20-ST) Microscope and analyzed using ImageJ software. The sizes of the SNPs are reported as the mean diameter ± standard deviation of the measurements.

Detection of Hg (II) with SNPs-Cy NH_2: For the evaluation of Hg (II) detection by the SNPs-$CyNH_2$ sensor, a 500 µM Hg (II) stock solution was prepared in an acidic medium (0.25% HNO_3 solution) from which adequate dilutions were made for each pattern whose concentration range is from 0 – 20 µM.

a) Initial protocol: 700 μL of SNPs-CyNH2, 770 μL of ultrapure water and 30 μL of Hg (II) solution in nitric acid (0.25% HNO_3 solution) were placed in a 2 mL microtube. The mixture was stirred for 20 seconds and after 5 min the sample was measured in the spectrophotometer, scanning between 300 and 700 nm.

b) Optimized protocol: For the tests, 2 mL microtubes were used in which the test components were added in the following order: 600 μL of the SNPs-CyNH2x10, 870 μL of ultrapure water and 30 μL of the Hg (II) solution in 0.25% HNO_3, the mixture was stirred for 20 seconds and allowed to react for 2 minutes, then the sample was measured in the spectrophotometer, scanning between 300 and 700 nm. "1X" was defined as the concentration of SNPs-CyNH2corresponding to an absorbance of 0.5 at 395 nm.

Hg (II) detection with SNPs-Cy: For the evaluation of Hg (II) detection by the SNPs-Cy sensor, a stock solution of 500 µM Hg (II) in 0.25% HNO_3 was prepared, from which adequate dilutions were made for each pattern whose concentration range goes from 0 – 5 µM.

a) Initial protocol: It was placed in a 2 mL microtube: 700 μL of the NPs, 770 μL of ultrapure water and 30 μL of Hg (II) solution in 0.25% nitric acid. The mixture was stirred for 20 seconds and the sample was subsequently measured in the spectrophotometer, scanning between 300 and 700 nm.

b) Optimized protocol: For the tests, 2 mL microtubes were used in which the test components were added in the following order: 600 μL of SNPs-Cy x10, 785 μL of ultrapure water, 100 μL of

phosphate buffer pH 8 (0.1 M) and 15 μL of the Hg (II) solution in 0.25% HNO_3, the mixture was stirred for 20 seconds and left to react for 20 minutes, then the samples were measured in the spectrophotometer, scanning between 300 and 700 nm. "1X" was defined as the concentration of SNPs-Cy corresponding to an absorbance of 0.5 at 395 nm.

2.2. Interfering study

For the assay, 1 mM solutions of Ca^{2+}, Mg^{2+}, Zn^{2+} with salts were prepared, from which aliquots would be taken for each trial. The study of the interferents was carried out using the method of presence and absence of Hg (II). The procedure for this test is the same as the protocols for each sensor, with the exception that the amount of ultrapure water is reduced and replaced by the salt solution, which is added at the end of each process. That is, they maintain the following order: SNPs-functionalized, ultrapure water, pH 8 buffer (for SNPs-Cy), Hg (II) solution (or 0.25% HNO_3 solution, for the blank) and solution of the salt to be evaluated.

2.3. Detection of Hg (II) in real water samples

Two real water samples were evaluated, which were called water 1 (Khor Al-Zubair port, Iraq) and water 2 (Shatt Al-Basra canal, Iraq), which were characterized by conductivity and pH measurements. For this study, the protocol described above was used for each sensor with the exception that the content of ultrapure water was reduced and replaced by spring water.

3. Results

3.1. Synthesis and characterization of SNPs using UV-Vis spectroscopy

SNPs were synthesized using the protocol described in previous sections. It was observed that when $NaBH_4$ was added, the solution acquired an intense yellow coloration characteristic for spherical SNPs. The SNPs after being functionalized and washed are shown in figure 1 (Inset).

3.2 Characterization of SNPs

3.2.1 Characterization of SNPs by UV-Vis spectrometry: The characterization was carried and results show in the UV-Vis spectrum (Figure 1). In fig. 1 shows the plasmonic resonance band, which has its maximum at 394 nm. For the method used, based on the reduction of $AgNO_3$ with $NaBH_4$, spherical SNPs with an average diameter of 50 nm and a plasmonic resonance band that appears around 400 nm have been previously reported [8]. SNPs functionalized with cysteamine **(**SNPs-CyNH2**)** are, shown in figure 1, in which the maximum of the plasmonic resonance band is found at 395 nm and 392 nm for SNPs functionalized with cysteine **(** SNPs-Cy)

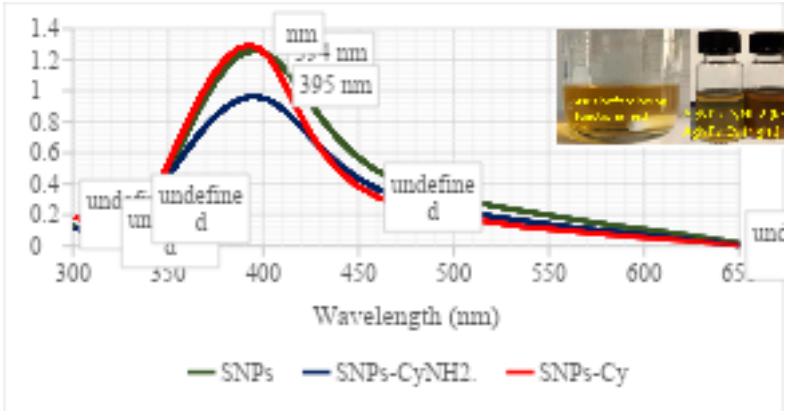

Figure 1: UV-Vis Spectrum of SNP; SNPs-CyNH$_2$; SNPs-Cy.

3.2.2. Transmission Electron Microscopy (TEM): The TEM characterization was carried out and obtained the images shown in figure 2 (a, b). The diameter size distribution graph shown in figure 2c. The average diameter turned out to be 30±2 nm.

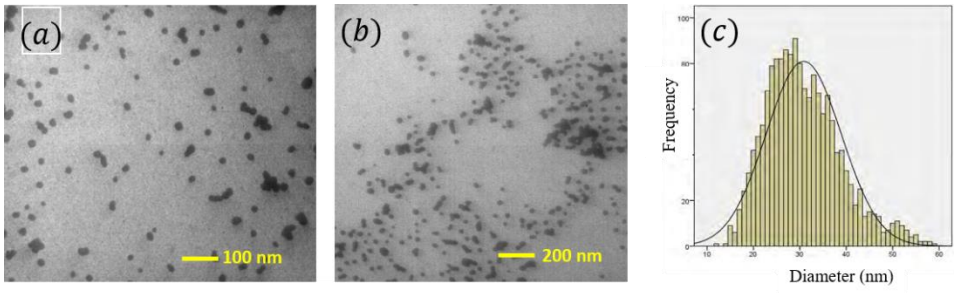

Figure 2: TEM images of SNPs-CyNH2a) 100 nm scale and b) 200 nm scale and (c) Histogram of the diameter distribution of the SNPs-CyNH2obtained by TEM images.

3.3. Detection of Hg (II) with SNPs functionalized with CyNH2 and Cy

Before optimizing the colorimetric sensor based on SNPs-CyNH2, preliminary tests were carried out to test the response and selectivity of the sensor against Hg (II). First, the detection of Hg (II) by unwashed SNPs-CyNH2 (SNPs-CyNH2_UW) was evaluated. The resulting spectra are shown in figure 3, in which it is observed that there is no significant response to the presence of Hg (II) by the SNPs-CyNH2_UW. This result would indicate that the SNPs-CyNH2_UW would not be interacting with Hg (II), since the excess ligand in solution would not allow the SNPs and mercury to interact [13].

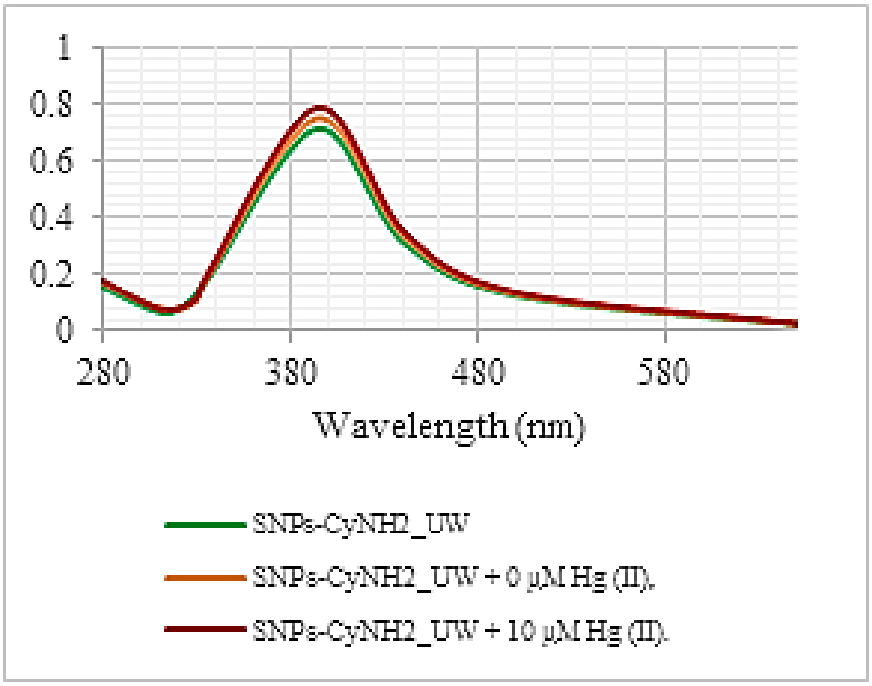

Figure 3: UV-Vis spectrum of SNPs-CyNH2_UW, SNPs-CyNH2_UW + 0 µM Hg (II), SNPs-CyNH2_UW + 10 µM Hg (II).

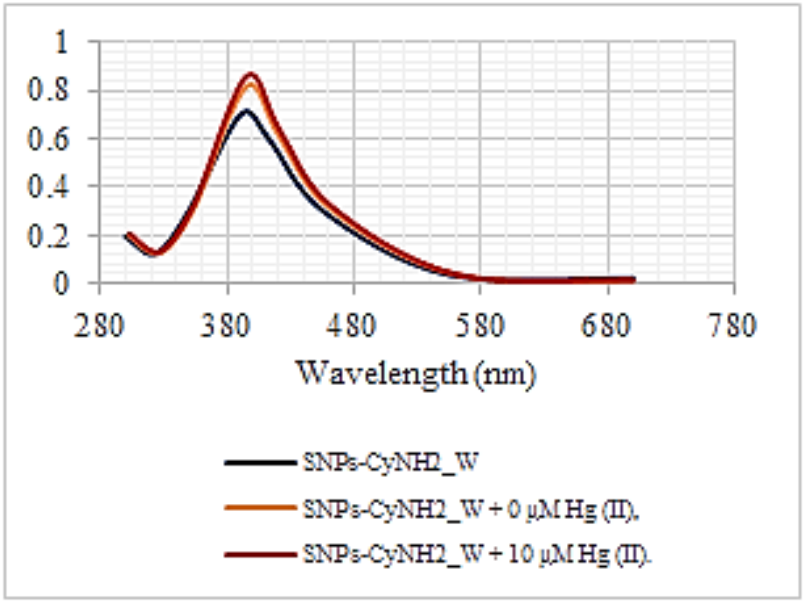

Figure 4: UV-Vis spectrum of SNPs-CyNH2_W, SNPs-CyNH2_W + 0 µM Hg (II), SNPs-CyNH2_W + 10 µM Hg (II).

Then, the detection of Hg (II) by the washed SNPs-CyNH2 (SNPs-CyNH2_W)(Figure 4) was evaluated, in which it is observed that there is a significant decrease in the plasmonic band and a displacement of the same towards shorter wavelengths (~~Bathochromic~~ shift). This result would indicate that the sensor based on SNPs-CyNH2 presents a specific response that can determine the amount of Hg (II) [14].

To study the stability and selectivity imparted by SNPs-CyNH2, tests were carried out in the presence of different concentrations of Ca^{+2}, the most important cation responsible for the so-called water hardness (along with Mg^{+2}). Results show that for non-functionalized SNPs from 0.5 mM of Ca^{2+} there is a decrease in the intensity of the plasmonic band, which falls completely at 1 mM of Ca^{2+}. In contrast, the SNPs-$CyNH_2$ support up to a concentration of 5 mM of Ca^{2+} without significant variations in the plasmonic band, both in intensity and shift in its wavelength. Finally, the behavior of SNPs (unfunctionalized) and SNPs-$CyNH_2$ at different pHs (4, 6 and 8) was studied. To carry out the tests at pH 4, the pH was adjusted with 0.1 M HCl, while for pHs 6 and 8 the pH was adjusted with 0.1 M phosphate buffer. The following UV-Vis spectra were obtained, shown in figures 5 and 6.

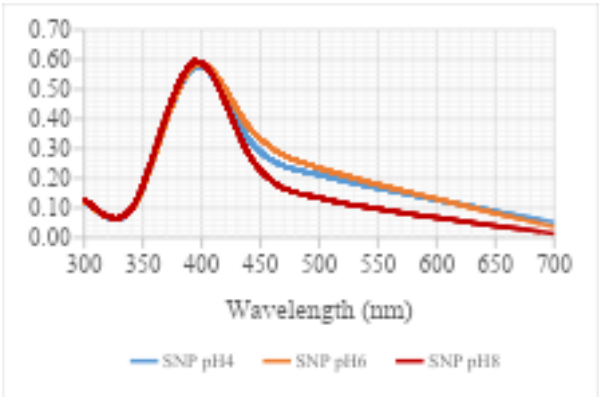

Figure 5: UV-Vis spectrum of SNPs at different pH values

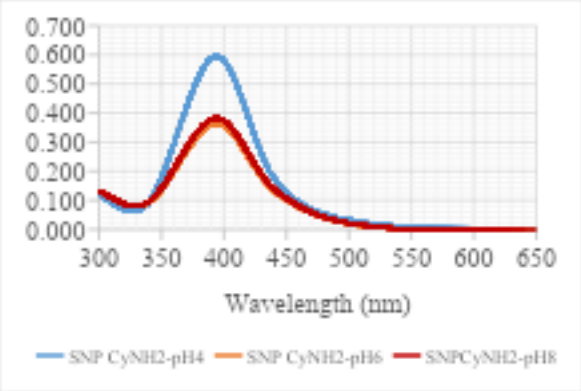

Figure 6: UV-Vis spectrum of SNPs-CyNH2 at different pH values.

Figures 5 and 6 show that the SNPs do not present any variation in the plasmonic band in response to the change in pH that causes a change in the ionic strength, since they are surrounded by the double electrical layer that forms the water around the SNPs. SNPs. On the other hand, SNPs-CyNH2, only the plasmonic band remains when they are at pH 4, as described by Mukherjee et [6] because in acid media SNPs-CyNH2 are dispersed while in basic media they aggregate due to the formation of hydrogen bonds [15].

On the other hand, unwashed SNPs-Cy (SNPs-Cy_UW) were also evaluated in the presence of Hg (II), in which it is observed that there is no significant response to Hg (II). This would indicate that SNPs-Cy_UW would not be interacting efficiently with Hg (II) due to excess ligand in solution, since the excess ligand would not allow interaction between SNPs and Hg (II). Subsequently, the detection of Hg (II) with the washed SNPs-Cy (SNPs-Cy_W) was evaluated. In which it is observed that there is a significant decrease in the plasmonic band, in addition to the appearance of a second curve around 650 nm, which indicates the aggregation of the SNPs. When the SNPs-Cy_W interact with Hg (II), the carboxyl and amino groups form a complex with mercury in such a way that it allows the aggregation of the SNPs-Cy as described in the work by [16]. The results of the evaluation of detection of Hg (II) with SNPs functionalized with cysteine, at pHs of 6, 7 and 8 using 0.1 M phosphate buffer are shown in figure 7.

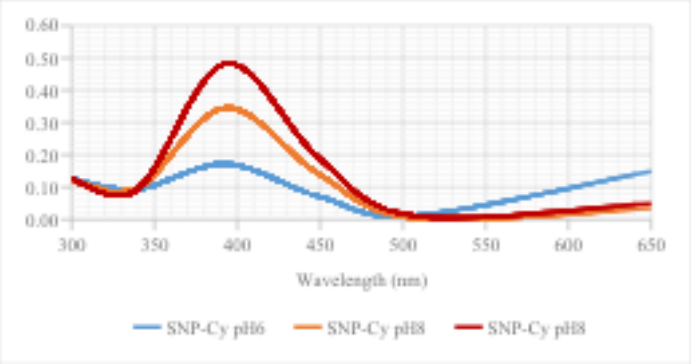

Figure 7: Spectra of SNPs-Cy at different pH values.

Figure 7 shows that there is aggregation of the SNPs-Cy at pH 6 and 7, which is not observed when using the buffer at pH 8. Therefore, for the subsequent tests, a buffer at pH 8 was used the carboxyl groups are negatively charged (pKa=1.96) and the amino groups (pKa=8.18) are not charged, so there are no electrostatic interactions or formation of hydrogen bonds between the amino and carboxylate groups that induce aggregation. Non-functionalized SNPs were evaluated in a final concentration of 2 μM Hg (II) solution, in which it is observed that there is no clear response of the plasmonic band.

3.4. Hg (II) Detection Assay Optimization

3.4.1. Evaluation of the amount of ligand

This test was carried out within the optimization process of the SNPs-CyNH2 and SNPs-Cy sensor for the detection of Hg (II), the effect of the amount of ligand on the plasmonic band was evaluated and results were given in figure 8

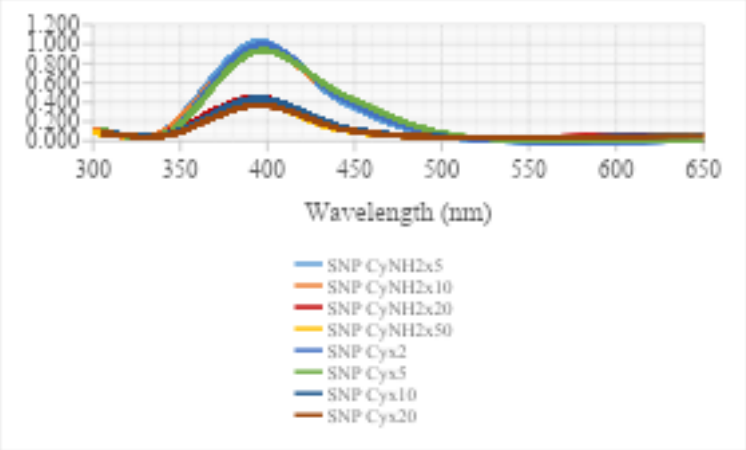

Figure 8: UV-Vis spectra of SNPs-CyNH2 and SNPs-Cy with different amounts of ligand.

In figure 8, it is observed that the SNPs-CyNH2×10 present a good intensity of the plasmonic band as well as SNPs-CyNH2x5, with the difference that SNPs-CyNH2×10 is more stable over time. In addition, a small increase in the band for SNPs-CyNH2 ×5 is observed in the 500-650 nm range, which could indicate that SNPs are aggregating. For larger amounts of ligand (×20, ×50), the band decreases its intensity and widens, due to the excess of ligand that can give rise to the agglomeration of the SNPs, that is, that the silver SNPs begin to associate forming larger particles large, causing a wide distribution of SNPs that causes the band to widen. Therefore, SNPs-CyNH2×10 were chosen for the other measurements. Figure 8 also shows that the SNPs-Cy×10 have a good intensity of the plasmonic band as SNPs-Cyx5, with the difference that the latter is less stable over time, since the SNPs-Cy×5 are grouped and precipitate, small gray particles being observed at the bottom of the container. Therefore, SNPs-Cy×10-chosen for the other tests.

3.4.2. Effect of the amount of SNPs-CyNH2 and SNPs-CyN in the detection of Hg (II)

The effect of the amount of SNPs-CyNH2×10 (1X, 1.5X and 2X) was evaluated, following the protocol described in section 5.2.6. The results shown in Figure 9 were obtained.

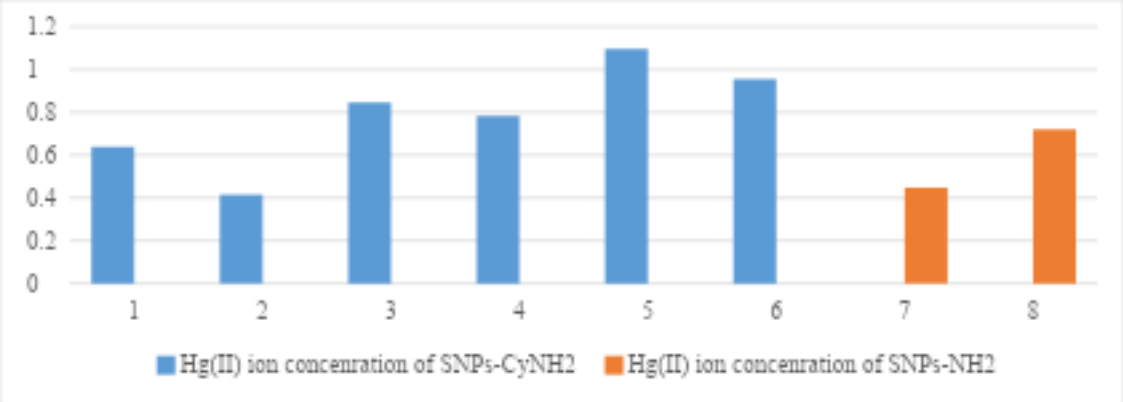

Figure 9: Graph of the effect of the amount of SNPs-CyNH2×10 for the detection of Hg (II) and the amount of AgNPs-Cyx10 on the detection of Hg (II) ion

From Figure 9 a similar response (signal decrease) can be observed for the three amounts of SNPs-CyNH2×10in the assay. 1.5X was chosen for the subsequent tests, because it presents an adequate intensity of the plasmonic band that allows observing the changes when the concentration of Hg (II) varies, in addition to presenting a small error. 1X was not chosen due to higher sensor saturation. Figure 9 (red color bars) shows the effect of the amount of SNPs-Cy on the detection of Hg (II) that 1X of SNPs-Cy×10 saturates from 1 μM of Hg (II). To perform the analysis, it is necessary to have a greater saturation range for the SNPs-Cy sensor, for this reason 1.5X was chosen since it also presents small errors and allows the detection range to be extended for different amounts of Hg (II) to be evaluated.

3.4.3. Evaluation of the incubation time for the detection of Hg (II)

For the evaluation of the incubation time, relatively long times (5, 10, 20 and 30 min) were taken first for 0, 5 and 20 μM of final concentration of Hg (II) using SNPs-CyNH2 and 0.5 SNPs-Cy sensor . The results are shown in Figure 10.

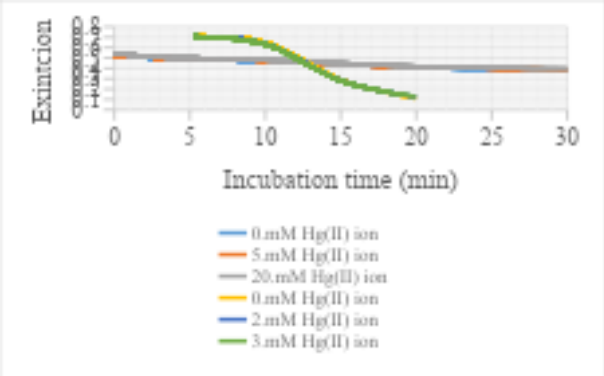

Figure 10: Graphs of Hg (II) concentration versus extinction, for times 5, 10, 20 and 30 min for the SNPs-CyNH2and 5, 10, 15 and 20 min for theSNPs-Cy Sensor .

Figure 10 shows that for all incubation times the response is the same for different concentrations of Hg (II), but as the concentration of Hg (II) increases, the error increases. Therefore, shorter incubation times were tested: 1, 3 and 5 min. The results are shown in figure 10. Figure 10 shows that, for all incubation times, the response is very similar to the different concentrations of Hg (II), in addition to increasing the concentration of Hg (II), the error remains small. Therefore, for convenience in the preparation of each measurement test, 2 minutes was defined as the optimal incubation time. On the other hand, at 20 min the variations are small and for times greater than 20 min no significant difference is observed, so 20 min was chosen as the optimal time for the SNPs-Cy Sensor.

3.5. Hg (II) calibration curve for the SNPs-CyNH2sensor by UV-Vis spectrophotometry

For the realization of the calibration curve, the previously established parameters were used, such as: amount of ligand to be used in theSNPs-CyNH2×10, amount of NPs of 1.5X and incubation time of 2 minutes. Measurements were performed in triplicate. The results are shown in figure 23.

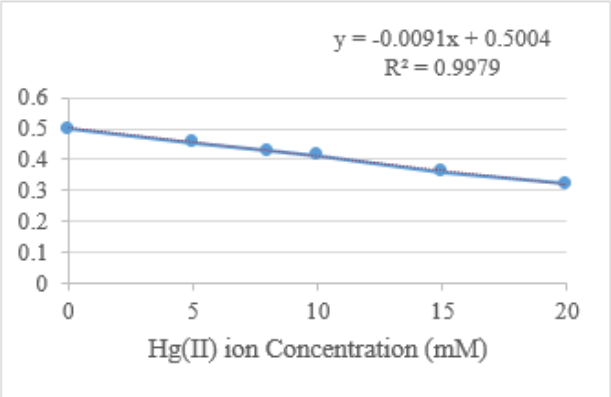

Figure 23: Hg (II) calibration curve for the SNPs − $CyNH_2$ × 10 sensor.

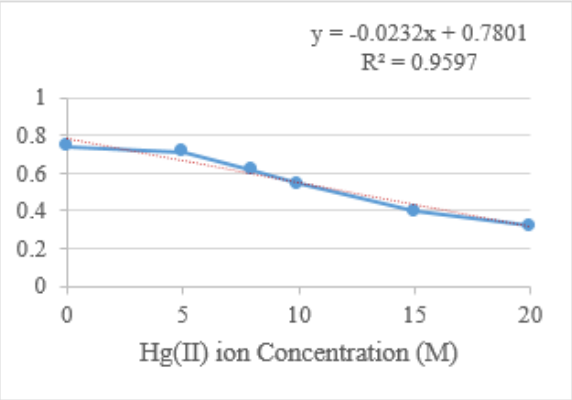

Figure 33: Hg (II) calibration curve for the SNPs-Cy× 10 sensor.

From the results shown in Figure 23, it can be seen that the curve has a linear trend. Applying linear regression to the data, the equation of the straight line and the detection limit of the SNPs-CyNH2x10 sensor for Hg (II) were determined. Taking into account three times the standard deviation of the 0 µM concentration of Hg (II), a detection limit value of 109 nM is obtained. For the realization of Hg (II) calibration curve for the SNPs-Cy sensor by UV-Vis spectrophotometry, the previously established parameters were used, such as the amount of ligand in the SNPs-CyNH2x10, amount of NPs of 1.5x and incubation time of 20 minutes. Measurements were performed in triplicate. The results are shown in figure 33. From the results shown in Fig. 33, it can be seen that the curve exhibits poor linearity. The detection limit of the SNPs-Cy×10 sensor for the detection of Hg (II) was estimated, taking into consideration three times the standard deviation of the 0 µM concentration of Hg (II). A detection limit value of 445 nM was obtained.

3.6. Evaluation of the detection of Hg (II) in the presence of interfering ions

Interfering ions were evaluated following the procedure described in earlier sections. To evaluate the response of the SNPs-CyNH2/SNPs-Cy sensor against Hg (II) in the presence of some ions commonly found in water such as cations like Ca, Mg, Ni, Cu) and anions like carbonates, chlorides, this assay was performed using the method of absence and presence of Hg (II) for a final concentration of 20 µM and-5 µM in case of SNPs-Cy sensor A concentration of the interfering salts of 133 µM and 20 µM of SNPs-Cy sensor was used for each of them, taking into consideration the concentration of the ions that give hardness to the water, which are calcium and magnesium. In the case of magnesium, lower concentrations were evaluated, but the same results were observed. The results are shown in figure 11. It is observed that the SNPs-CyNH2/SNPs-Cy sensor is quite selective for most of the ions evaluated, except for the magnesium ion, which presents a similar response to mercury.

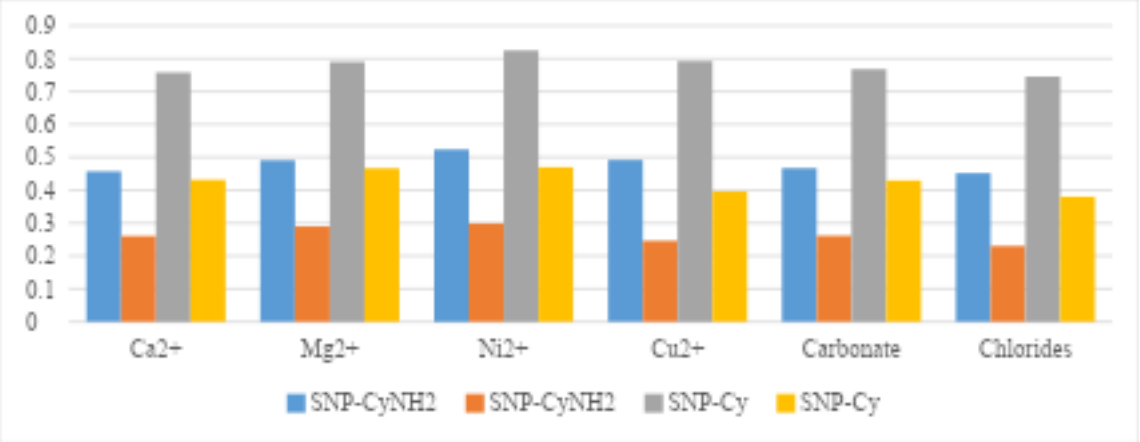

Figure 11: Bar chart of different salts used as interferents in the detection of Hg (II).

3.7 Hg (II) detection test in real water samples

The test was carried out following the procedure described in section 5.2.9 to evaluate the use of the sensor based on SNPs-CyNH2/SNPs-Cy to detect Hg (II) in real water samples collected from the two locations water 1 & water 2 having the electrical conductivity (μS/cm) 736±1 & 105.9±0.1 and pH 7.75±0.01& 7.18±0.01 respectively. The results of the test to detect Hg (II) with the sensor based on SNPs-CyNH2/SNPs-Cy in real water samples are shown in Figure 12. 60 μL of water 1 and 750 μL of water 2 were used.

Figure 12 shows that the response of the SNPs-CyNH2/SNPs-Cy sensor in ultrapure water is very similar for both spring water 1 and spring water 2, which is a good sign since the sensor responds appropriately in media other than the ultrapure water test. It should be noted that different amounts of spring water were used in the tests due to the different content of dissolved salts in each sample. On the other hand, it is observed that the errors are small both for the zero and for the samples with Hg (II).

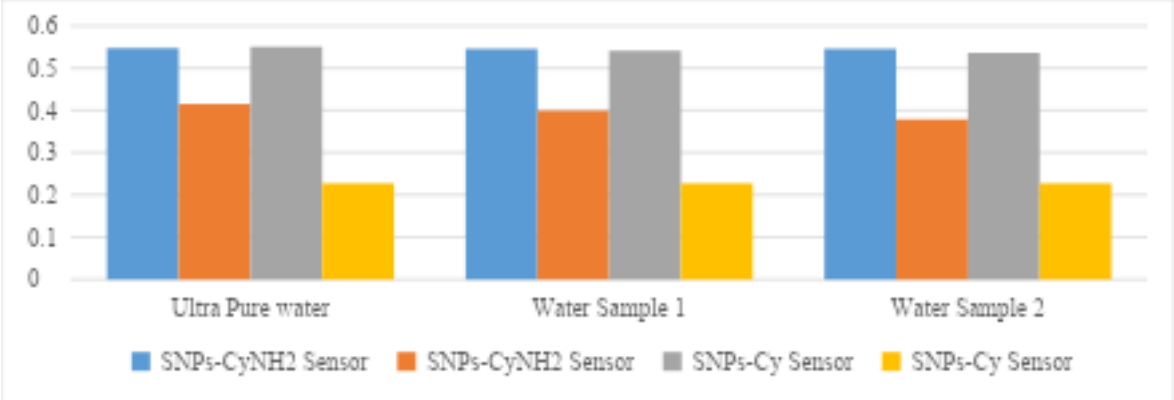

Figure 12: Comparison of the response to Hg (II) detection by the SNPs-CyNH2/SNPs-Cy **sensor in real water samples at 0, 20, 5μM concentration of Hg (II) ion**

The test results are shown in Figure 12.75 µL of spring water 1 and 750 µL of spring water 2 were used in the test. It should be noted that different amounts of spring water were used in the tests due to the different content of dissolved salts in each sample. It is observed that the response of the SNPs-Cy sensor for 0 Hg (II) is within the experimental error for all the samples, in addition, no appreciable effect of the matrix is observed. On the other hand, a slight variation of the sensor response is observed in the presence of Hg (II).

4. DISCUSSION OF RESULTS

4.1. Synthesis and characterization of SNPs

Given the objectives of this work, it was based on three main stages: the synthesis of SNPs, functionalization of SNPs with short sulfur ligands and their subsequent use in the detection of Hg (II) in water. To carry out the synthesis, the modified process of the Creighton method [17] was used, in which $AgNO_3$ is used as the precursor of the SNPs and $NaBH_4$ as the reducing agent. Spherical SNPs with an average size of 31±8 nm were obtained according to the analysis of TEM micrographs. The maximum of the plasmonic band appeared between 395±3 nm for different batches, which is consistent with the references that indicate that the plasmonic band for spherical SNPs appears around 400 nm.

The reaction for the synthesis of SNPs is carried out by means of the chemical reaction [5, 6]:

$$AgNO_3 + NaBH_4 \rightarrow Ag + 1/2\ H_2 + 1/2\ B_2H_6 + NaNO_3$$

The reduction of Ag ions by sodium borohydride is initially very fast, especially when it is in excess. For this reason, the speed and uniformity in the agitation, as well as the temperature control (keeping the temperature low) have effects on the LSPR band, being able to make it wide and not very intense when the synthesis is carried out at room temperature. Furthermore, it has been reported that the size and morphology of SNPs depend on various parameters such as the ratio between silver and borohydride, pH and light exposure. Therefore, the production of SNPs is very sensitive to the preparation conditions, so the Ag colloids were prepared with extreme care and under controlled conditions of temperature, pH, light protection and stirring speed.

4.2. Functionalization of SNPs with short sulfur ligands

The functionalization process of the SNPs with $CyNH_2$ was carried out as described in section 5.2.2. The pH of the SNPs was adjusted from their initial pH of around 9 to a pH of 4 before adding the ligand. The pH of the colloid after the addition of the ligand was 4. The results show that the SNPs-CyNH2 aggregate at pHs greater than 6. On the other hand, as reported by Rajkumar et [5], the union occurs through the interaction of the thiol groups of the $CyNH_2$ with the surface of the SNPs, this interaction is of the chemisorption type. SNPs-CyNH2 are able to resist Ca^{2+} solutions at concentrations of 5 mM while SNPs (unfunctionalized) become unstable at concentrations greater than 0.5 mM. The functionalization process of the SNPs with Cy was carried out as the final pH of the colloid was 8, due to the fact that during the process of removing excess ligand it was necessary to adjust the washing water to pH 8, since SNPs-Cy add at a pH lower than 8. Because the pKa of the amino group has a value of 8.18 and in an acid medium it is protonated, which can form hydrogen bonds and make the SNPs aggregate. These results are different from those obtained by Rajkumar et al. [5] because in their work they did not observe aggregation at acidic pH, they only observed a small shift of the band towards shorter wavelengths as the pH increased.

4.3. Detection of Hg (II) with functionalized SNPs

Incubation time and amount of SNPs-CyNH2, observing a favorable response in the detection of Hg (II). This protocol was improved and optimized to be able to use the sensor in the quantification of Hg (II). The optimization of the SNPs-CyNH2 sensor for the detection of Hg (II) was carried out by evaluating the following parameters: a) amount of ligand, b) amount of SNPs-CyNH2x10 and c) Incubation time in the detection of Hg (II). With the optimized protocol, a calibration curve was made by UV-Vis spectrophotometry.

The SNPs-CyNH2 sensor showed a detection limit of 109 nM and a linear range between 0 and 20 μM Hg (II). An explanation of the mechanism of the interaction between SNPs-CyNH2 and Hg (II) has been given by Chakraborty et al.[6] in which an exchange of the ligand between SNPs and Hg (II) would occur, which is thiophilic, deprotecting the surface of SNPs and leaving it exposed for

the redox reaction to occur between Ag and Hg (II). This reaction gives rise to the formation of a nanoalloy (nanoamalgam) that causes a change in the LSPR band. The reaction between SNPs and Hg (II) would occur as follows [6]:

$$Agn + Hg^{2+} \rightleftharpoons Agn{-}2Hg + 2Ag^{+}$$

The process that gives rise to the Ag@Hg nanoalloys takes place in the following steps: first, rapid adsorption of the Hg atoms on the SNPs; second, rapid diffusion of Hg atoms within the SNPs; third, a greater diffusion of Hg atoms that leads to the formation of Ag and Hg uniformly distributed in spherical Ag@Hg nanoalloys. On the other hand, to carry out the detection of Hg (II) with the SNPs-Cy sensor, the use of a buffer at pH 8 was required because, the SNPs-Cy when exposed to a slightly acidic or neutral medium added , because the amine of Cy takes its positive ionic form, which facilitates the formation of hydrogen bonds with the carboxylic groups of other molecules and the SNPs agglomerate [14]. The fact that the SNPs-Cy precipitated in an acidic medium was presented as a drawback since the Hg (II) solutions were in an acidic medium (0.25% HNO_3 solution). For the optimization of the SNPs-Cy sensor in the detection of Hg (II), the following parameters were evaluated: a) the amount of ligand to be used b) the amount of SNPs-Cyx10 and c) the incubation time. With the optimized protocol, a calibration curve was obtained. The SNPs-Cy sensor showed a detection limit of the order of 440 nM and a detection range between 0 and 5 μM Hg (II), which is the concentration at which the sensor saturates, with low linearity. Rajkumar et al [5] have reported an Hg (II) sensor based on SNPs-Cy. In this study, the LSPR band progressively disappears in the presence of the analyte and the proposed mechanism is analogous to that of the sensor based on SNPs-CyNH2 previously described (formation of a silver amalgam). This report differs from the results shown in this work, which show the aggregation of SNPs in the presence of Hg (II) through the appearance of a second peak around 650 nm. This difference may be due to the synthesis process since Rajkumar [6] adds Cy to the $AgNO_3$ solution and then adds this mixture to the $NaBH_4$ solution; On the other hand, it should be noted that he uses 3.3 times less ligand than we do, and does not carry out any washing process to eliminate excess ligand. At the assay pH (around 8), the cysteine carboxyl group (isoelectric point 5.0728) is deprotonated, stabilizing the SNPs-Cy, free to interact with the analyte.

On the other hand, the review presented by Balme et.[9] and the work by Haibin Li et .[10] show how SNPs-Cy interact with mercury through an aggregation mechanism, where through chemisorption-type interactions, SNPs aggregate through the carboxylate group of Cy with the metal ion, in the ratio of two Cy for each metal ion, which would be consistent with the appearance of a second peak around 650 nm and the color change from yellow to violet blue and later colorless product of aggregation. Greater detail between the interaction of SNPs-Cy and Hg (II) has been reported by Zhan et al.[11], in which it is observed how the amino and carboxylate groups of cysteine bind to Hg (II)

In the case SNPs-CyNH2, good results were generally obtained for all the interfering ions studied, with the exception of magnesium, with which it was observed that there was a response from the sensor in the absence of Hg (II). This fact can be explained due to the interactions between the SNPs-CyNH2 and magnesium, due to the stability tendencies of the metallic complexes by the amines of the $CyNH_2$, which would behave as hard bases for which they would present greater affinity for a hard acid such as the Mg^{2+} ion rather than a soft acid such as Hg (II). The response by magnesium would limit the use of the sensor in hard water, since it would have a high content of calcium and magnesium. For the SNPs-Cy sensor, interference was observed due to the poor selectivity of the carboxyl and amino groups of cysteine. Response was observed for Cu and Ni. This behavior can be explained due to the chelate effect of the amino and carboxylate groups against said metals. Cu^{2+} and Ni^{2+} ions are acids with intermediate behavior, that is, they can act as hard or soft acids depending on the ligand with which they are interacting.

5.0 Conclusions and recommendations

The protocol for the synthesis of spherical SNPs was standardized by the modified process of the Creighton method. SNPs with an average diameter of 30±2nm were obtained according to the characterization by analysis of the TEM images. A functionalization protocol for SNPs with cysteamine and cysteine ligands for the detection of Hg (II) in water was implemented and optimized. A protocol for the quantification of Hg (II) in water by UV-Vis spectrophotometry was established and optimized for each sensor under study. It was possible to obtain a detection limit of 109 nM for the SNPs-CyNH2sensor with an incubation time of 2 min and a detection limit of 445 nM for the SNPs-Cy sensor with an incubation time of 20 min. On the other hand, although it has not been possible to detect quantities of Hg (II) below the detection limits established by the regulatory entities, it has been possible to develop a simple, practical and rapid methodology for the detection of Hg (II). The sensor based on SNPs-CyNH2present's good selectivity for most of the interfering ions studied. On the other hand, the SNPs-Cy sensor has limited selectivity due to the cysteine functional groups that are not very selective and induce aggregation with metal ions such as Cu^{2+} and Ni^{2+}. In addition, it should be noted that both sensors support a limited hardness. It is recommended to evaluate the elimination of the interferents that affect each sensor to avoid false positives in the analyses and reduce hardness through the use of ion exchangers known as softeners, which replace calcium and magnesium ions with other ions such as sodium or potassium. It is recommended to evaluate the Hg (II) detection methodologies studied so that they can be adapted to portable UV-Vis spectrophotometry systems and field trials can be carried out in situ.

References

1. Min Xia Quan, Qing Feng Yao, Qing Yu Liu, Zhen Qi Bu, Xue Zhi Ding, Li Qiu Xia, Jiao Yang Lu, Wei Tao Huang. Microwave-Assisted Synthesis of Silver Nanoparticles for Multimode Colorimetric Sensing of Multiplex Metal Ions and Molecular Informatization Applications. ACS Applied Materials & Interfaces 2022, 14 (7) , 9480-9491.
2. Akashdeep Nath, Gegari M Thomas, Shivali Hans, Sivaranjana Reddy Vennapusa, Sukhendu Mandal. Crystal Packing-Driven Selective Ion Sensing Using Thiazolothiazole-Based Water-Stable Zinc Metal–Organic Framework. Inorganic Chemistry 2022, 61 (4) , 2227-2233.
3. Prioti Choudhury Purba, Mangili Venkateswaralu, Soumalya Bhattacharyya, Partha Sarathi Mukherjee. Silver(I)–Carbene Bond-Directed Rigidification-Induced Emissive Metallacage for Picric Acid Detection. Inorganic Chemistry 2022, 61 (1) , 713-722
4. Jian Wang, Yahong Zhou, Lei Jiang. Bio-inspired Track-Etched Polymeric Nanochannels: Steady-State Biosensors for Detection of Analytes. ACS Nano 2021, 15 (12) , 18974-19013
5. Nidya, M.; Umadevi, M.; Rajkumar, B. J. M. Structural, Morphological and Optical Studies of l-Cysteine Modified Silver Nanoparticles and Its Application as a Probe for the Selective Colorimetric Detection of Hg2+. Spectrochim. Acta - Part A Mol. Biomol. Spectrosc. 2014, 133, 265–271
6. Bhattacharjee, Y.; Chakraborty, A. Label-Free Cysteamine-Capped Silver Nanoparticle-Based Colorimetric Assay for , Detection in Water with Subnanomolar Exactitude. ACS Sustain. Chem. Eng. 2014, 2, 9, 2149–2154.
7. Creighton, J. A.; Blatchford, C. G.; Albrecht, M. G. Plasma Resonance Enhancement of Raman-Scattering by Pyridine Adsorbed on Silver or Gold Sol Particles of Size Comparable to the Excitation Wavelength. J. Chem. Soc. Trans. Ii 1979, 75, 790–798.
8. Ravindran A., Priya S., Chandrasekaran N., Mukherjeea A. Differential interaction of silver nanoparticles with cysteine. Journal of Experimental Nanoscience 2013.8, 4, 589–595.

9. Sabela, M.; Balme, S.; Bechelany, M.; Janot, J. M.; Bisetty, K. A Review of Gold and Silver Nanoparticle-Based Colorimetric Sensing Assays. Adv. Eng. Mater. 2017, 19, 12, 1-7.
10. Li, H.; Bian, Y. Selective Colorimetric Sensing of Histidine in Aqueous Solutions Using Cysteine Modified Silver Nanoparticles in the Presence of Hg2+.Nanotechnology 2009, 20, 14, 145502.
11. Duan, J.; Zhan, J. Recent developments on nanomaterials-based optical sensors for Hg2+ detection. Science China Materials 2015. 58, 3, 223-240.
12. Anupam Manna, Ashish Kumar Maharana, Gugulothu Rambabu, Sagarika Nayak, Suddhasatwa Basu, Sanjib Das. Dithia-Crown-Ether Integrated Self-Exfoliated Polymeric Covalent Organic Nanosheets for Selective Sensing and Removal of Mercury. ACS Applied Polymer Materials 2021, 3 (11) , 5527-5535.
13. Xinfeng Zhang, Hao Hu, Weiwei Liu, Yanying Wang, Juewen Liu, Peng Wu. Selective Heavy Atom Effect Forming Photosensitizing Hot Spots in Double-Stranded DNA Matrix. The Journal of Physical Chemistry Letters 2021, 12 (38) , 9205-9212.
14. Jie Zhang, Qiguang Zang, Fulin Yang, Haoke Zhang, Jing Zhi Sun, Ben Zhong Tang. Sulfur Conversion to Multifunctional (O-thiocarbamate)s through Multicomponent Polymerizations of Sulfur, Diols, and Diisocyanides. Journal of the American Chemical Society 2021, 143 (10) , 3944-3950
15. Neha Choudhury, Bhuban Ruidas, Chitrangada Das Mukhopadhyay, Priyadarsi De. Rhodamine-Appended Polymeric Probe: An Efficient Colorimetric and Fluorometric Sensing Platform for Hg2+ in Aqueous Medium and Living Cells. ACS Applied Polymer Materials 2020, 2 (11) , 5077-5085
16. Fei Chen, Rachel L. Warnock, Jan Roelof Van der Meer, Seraphine V. Wegner. Bioluminescence-Triggered Photoswitchable Bacterial Adhesions Enable Higher Sensitivity and Dual-Readout Bacterial Biosensors for Mercury. ACS Sensors 2020, 5 (7) , 2205-2210
17. Trefry, John & Fore, Jennifer & Weaver, Kent & Meyerhoefer, Allie & Markopolous, Marjorie & Arnold, Zachary & Wooley, Dawn & Pavel, Ioana. (2010). Size Selection and Concentration of Silver Nanoparticles by Tangential Flow Ultrafiltration for SERS-Based Biosensors. Journal of the American Chemical Society. 132. 10970-2. 10.1021/ja103809c.